

1

2

3 **Comparative analysis of transcriptomic profiles among**  
4 **ascidians, zebrafish, and mice: insights from tissue-specific**  
5 **gene expression**

6

7 Shin Matsubara\*, Tomohiro Osugi, Akira Shiraishi, Azumi Wada, Honoo Satake

8

9 Bioorganic Research Institute, Suntory Foundation for Life Sciences, Kyoto, Japan

10

11 **Short title:** Comparative analysis of transcriptomic profiles among ascidians, zebrafish, and  
12 mice

13

14

15 \* Corresponding author

16 E-mail: matsubara@sunbor.or.jp

17

18

19

20

21

22

23

24

25

26

27

28

29

30

## 31 Abstract

32 Tissue/organ-specific genes (TSGs) are important not only for understanding organ  
33 development and function, but also for investigating the evolutionary lineages of organs in  
34 animals. Here, we investigate the TSGs of 9 adult tissues of an ascidian, *Ciona intestinalis* Type  
35 A (*Ciona robusta*), which lies in the important position of being the sister group of vertebrates.  
36 RNA-seq and qRT-PCR identified the *Ciona* TSGs in each tissue, and BLAST searches  
37 identified their homologs in zebrafish and mice. Tissue distributions of the vertebrate homologs  
38 were analyzed and clustered using public RNA-seq data for 12 zebrafish and 30 mouse tissues.  
39 Among the vertebrate homologs of the *Ciona* TSGs in the neural complex, 48% and 63%  
40 showed high expression in the zebrafish and mouse brain, respectively, suggesting that the  
41 central nervous system is evolutionarily conserved in chordates. In contrast, vertebrate  
42 homologs of *Ciona* TSGs in the ovary, pharynx, and intestine were not consistently highly  
43 expressed in the corresponding tissues of vertebrates, suggesting that these organs have evolved  
44 in *Ciona*-specific lineages. Intriguingly, more TSG homologs of the *Ciona* stomach were highly  
45 expressed in the vertebrate liver (17-29%) and intestine (22-33%) than in the mouse stomach  
46 (5%). Expression profiles for these gene suggest that the biological roles of the *Ciona* stomach  
47 are distinct from those of their vertebrate counterparts. Collectively, *Ciona* tissues were  
48 categorized into 3 groups: i) high similarity to the corresponding vertebrate tissues (neural  
49 complex and heart), ii) low similarity to the corresponding vertebrate tissues (ovary, pharynx,  
50 and intestine), and iii) low similarity to the corresponding vertebrate tissues, but high similarity  
51 to other vertebrate tissues (stomach, endostyle, and siphons). The present study provides  
52 transcriptomic catalogs of adult ascidian tissues and significant insights into the evolutionary  
53 lineages of the brain, heart, and digestive tract of chordates.

54

55 **Keywords:** Tissue-specific gene; *Ciona intestinalis*; neural complex; heart; stomach; RNA-seq

56

57

58

59

60

61

62

63

64

65

## 66 Introduction

67 During the past two decades, genome assembly and phylogenetic analyses of *Ciona*  
68 *intestinalis* Type A (or *Ciona robusta*) have verified that ascidians belong to the Urochordata  
69 phylum, which are the closest living relatives to the Vertebrata phylum in the Chordata  
70 superphylum [1-3]. Due to their important phylogenetic position, ascidians have attracted  
71 attention as model organisms for evolutionary studies. Particularly, the simplicity of the larval  
72 body and experimental advantages of *in vitro* fertilization and embryogenesis have revealed  
73 various conserved features in the development of the central nervous system (CNS) [4-8].  
74 Moreover, recent single-cell analyses further detailed the cell fates reported in previous studies  
75 and revealed conserved gene regulatory networks during embryo development [7-9]. Such  
76 studies have underscored the morphological and developmental similarities between ascidian  
77 larva and vertebrates and provided significant insights into the evolutionary lineages of  
78 embryogenesis and morphogenesis in chordates [4-6].

79 Adult ascidians (or sea squirts) develop from swimming larvae via metamorphosis and 1<sup>st</sup>  
80 and 2<sup>nd</sup> ascidian stages in 2.5-3 months [10]. They are enveloped by a polysaccharide-containing  
81 tunic and intake water and food from an oral siphon (Fig 1) [11]. The pharynx serves dual roles  
82 as an apparatus for food collection and gas exchange with water (Fig 1) [11]. The endostyle is  
83 located at the ventral side and secretes mucus into the pharynx. The resultant food cord is  
84 transported to the stomach and intestine, and then excreted through the atrial siphon (Fig 1)  
85 [11]. Mature oocytes are produced in the ovary located beside the heart and are spawned from  
86 the atrial siphon via an oviduct (Fig 1) [11]. These peripheral tissues are regulated by the neural  
87 complex (Fig 1) [11]. In fact, we have identified more than 30 neuropeptides and visualized the  
88 entire neural network of adult ascidians using transgenic animal models [12-15]. In contrast,  
89 despite the growing body of knowledge regarding early embryos and larvae, less attention has  
90 been paid to the functions and evolutionary lineages of the adult tissues of ascidians.

91

92 **Fig 1. Schematic illustration of the body structure of an adult ascidian.** The illustration was  
93 modified from Osugi et al., 2020 [12]. The key anatomical parts of the 9 tissues analyzed in this  
94 study are indicated. AS, atrial siphon; Endo, endostyle; Int, intestine; NC, neural complex; OS,  
95 oral siphon; Ova, ovary; Pha, pharynx; Stom, stomach.

96

97 Cell types and functions in an organism are featured (or characterized) by specific gene  
98 expression. Thus, tissue-specific genes (TSGs) are important for tissue-specific function and/or  
99 development. In vertebrates, expression profiles for various TSGs are more conserved in the  
100 same or functionally related organs among different species than in other organs in the same

101 species [16-19]. Moreover, the speed of evolution is fast in paralogs but slow in orthologs  
102 [20,21]. Therefore, identification of TSGs in *Ciona* and comparison to their vertebrate  
103 homologs is expected to significantly contribute to the clarification of the evolutionary origin  
104 and functional lineages of the respective tissues in chordates. In *Ciona*, expressed sequence tag  
105 data during embryogenesis [22,23] and in young adults [24], and transcriptomes of young and  
106 adult ovaries and isolated ovarian follicles [25,26], are available. Moreover, microarray data for  
107 adult tissues have identified TSGs in 11 tissues and determined their chromosomal locations  
108 [27]. However, the lack of comparative analyses of *Ciona* TSGs with vertebrate homologs has  
109 hindered the understanding of the evolutionary implication in each tissue in chordates.

110 In this study, we present transcriptomic profiles for adult tissues of *Ciona intestinalis* Type  
111 A (or *Ciona robusta*) and identify the TSGs in each tissue. Searching for zebrafish and mouse  
112 homologs of the *Ciona* TSGs and analyzing their tissue distributions in zebrafish and mice  
113 uncovered gene expression similarities in each tissue among the species. Such comparative  
114 analyses of *Ciona* TSGs with their homologs in zebrafish and mice provide evolutionary  
115 insights into the biological functions of *Ciona* tissues.

116  
117

## 118 **Results and Discussion**

### 119 **Identification of TSGs in *Ciona***

120 To identify TSGs in *Ciona*, RNA-sequencing (RNA-seq) was performed using 11 samples  
121 of 9 tissues of adult ascidians (oral siphon, atrial siphon, neural complex, endostyle, heart,  
122 ovary, pharynx, stomach, and intestine). The raw sequence data were deposited into the NCBI  
123 database (PRJNA731286). Total reads, mapping rates, and accession numbers for each sample  
124 are listed in Table 1. The expression level for each gene was calculated as RPKM (reads per  
125 kilobase per million total reads) and is listed in S1 Table with raw read numbers. A previous  
126 microarray analysis identified TSGs based on the ratio of the median expression values between  
127 a specific organ and others (cutoff values ranging 1.3-9.4) [27]. Such median-based  
128 identification includes specifically expressed genes in individual and multiple tissues (e.g.,  
129 brain- and intestine-specific genes). To define tissue specificity more strictly, we identified  
130 TSGs based on the RPKM (RPKM > 1 in an individual tissue and RPKM < 0.5 in all other  
131 tissues, i.e., all TSGs show more than 2-fold higher expression than any other tissues) (Table 1  
132 and S2 Table). The RNA-seq data reproduced some of the specific expression patterns of the  
133 previously identified TSGs in the neural complex, endostyle, heart, ovary, stomach, and  
134 intestine (S1 Fig) [27], confirming the reliability of the RNA-seq data and their usefulness for  
135 the following analyses. The greatest number of TSGs was identified in the intestine (312 genes)

136 and the least was in the pharynx (15 genes) (Table 1). Amino acid sequences for the identified  
 137 TSGs in *Ciona* were subjected to BLASTP analysis against the RefSeq protein database for  
 138 mice and zebrafish using an e-value threshold  $< 1e-5$ . More than 50% of the TSGs in the  
 139 siphons (66 genes, 58.9%), neural complex (56 genes, 57.7%), heart (31 genes, 62.0%), ovary  
 140 (105 genes, 58.3%), and stomach (23 genes, 60.5%) were found to be homologous to the mouse  
 141 and/or zebrafish genes (Fig 2). On the other hand, 37 genes (56.1%) in the endostyle, 204 genes  
 142 (65.4%) in the intestine, and 12 genes (80.0%) in the pharynx had no homologous mouse or  
 143 zebrafish genes, suggesting that these tissues have *Ciona*-specific functions (Fig 2).

144

145 **Table 1. RNA-seq summary of adult *Ciona* tissues.**

Sample	Number of TSG	Total reads	% Mapped	Accession
Oral Siphon	112	28,379,690	94.92	SRR14597452
Atrial Siphon		22,999,973	94.92	SRR14597461
Neural Complex	97	23,236,898	89.91	SRR14597453
Endostyle	66	25,164,333	92.97	SRR14597460
Heart	50	22,512,838	91.20	SRR14597459
Ovary	180	23,763,137	94.48	SRR14597457
Pharynx	15	23,396,141	87.68	SRR14597458
Stomach	38	28,571,477	91.70	SRR14597456
Intestine (proximal)	312	24,346,598	91.20	SRR14597451
Intestine (middle)		26,999,786	89.67	SRR14597454
Intestine (distal)		26,160,308	89.46	SRR14597455

146 TSGs for the siphons and intestine include the genes with RPKM  $> 1$  either in the oral siphon or  
 147 atrial siphon and in any part of the intestine, respectively. The RNA-seq reads were mapped to the  
 148 *Ciona* cDNA library, and the mapping rates and accession numbers were shown.

149

150 **Fig 2. Number of genes homologous to the *Ciona* TSGs in mice and zebrafish.** Amino acid  
 151 sequences of the *Ciona* TSGs were blasted against the RefSeq protein database of mice and  
 152 zebrafish with the e-value set to  $< 1e-5$ . The number of genes homologous to mice (green),  
 153 zebrafish (yellow), or both (orange) in each tissue are shown. The genes without BLAST hits  
 154 are shown as non-homologous (blue). NC, neural complex.

155

## 156 **Similarity of gene expression patterns between *Ciona* TSGs** 157 **and their homologs in mice or zebrafish**

158 The tissue distributions of mouse and zebrafish genes homologous to the *Ciona* TSGs were  
 159 investigated. RNA-seq data using 17 mouse organs (30 tissues, PRJNA267840) and 12

160 zebrafish tissues (PRJNA255848) were obtained and expression levels were normalized from 0  
161 to 1. The number of highly expressed genes ( $> 0.8$ ) in each tissue was counted and the ratio was  
162 indicated as “tissue similarity” between *Ciona* and zebrafish or mice. Based on the tissue  
163 similarity, *Ciona* tissues were categorized into the following three groups. (i) TSG-rich tissues  
164 homologous to vertebrate counterparts: high similarity to the corresponding tissues in mice and  
165 zebrafish, (ii) *Ciona*-unique gene-rich tissues: low similarity to the corresponding and/or other  
166 tissues, and (iii) homologous TSG-rich tissues histologically unrelated to the vertebrate  
167 counterparts: low similarity to the corresponding tissues but high similarity to other tissues.

168

### 169 **(i) TSG-rich tissues homologous to vertebrate counterparts:** 170 **neural complex and heart**

171 The mouse (62.5%) and zebrafish (48.2%) homologs of *Ciona* neural complex-specific  
172 genes showed high expression in the corresponding mouse and zebrafish brains (Fig 3A),  
173 indicating that expression of the homologous genes in CNS tissues is highly conserved in the  
174 evolutionary lineage of chordates. Tissue distributions of the mouse and zebrafish homologs to  
175 *Ciona* TSGs were visualized as heat maps and clustered by their expression patterns (Fig 3B).  
176 Thirty-two mouse and 27 zebrafish homologs were included in the brain cluster (Fig 3B,  
177 orange). Gene ontology (GO) analyses indicated that 18 mouse and 12 zebrafish homologs have  
178 characteristic GO terms (biological process) for brain development or function (Fig 3B, *Ciona*  
179 IDs in red and S2 Table), and 6 genes of the genes (cholinergic receptors (*Chrn3* and *Chrm5*),  
180 gamma-aminobutyric acid (GABA) receptor (*Gabra6*), genes for synapse organization (*Mdga2*  
181 and *Nlgn1*) and brain differentiation (*Otp*)) were predominantly expressed in the brain of both  
182 species (Fig 3B, highlighted in yellow and S2 Table). Specific expression of the *Ciona*  
183 homologs (KY.Chr10.638, KY.Chr3.84, KY.Chr7.428, KY.Chr9.555, KY.Chr3.577, and  
184 KY.Chr14.946) of the 6 genes (*Chrn3*, *Chrm5*, *Nlgn1*, *Gabra6*, *Mdga2*, and *Otp*) in the neural  
185 complex was reproduced by qRT-PCR using 3-4 independent sets of the *Ciona* tissues from that  
186 used for RNA-seq (Fig 3C), confirming the reliability of RNA-seq data.

187

188 **Fig 3. Comparative analyses of *Ciona* TSGs in the neural complex and their homologs in**  
189 **mice and zebrafish.** (A) Similarities in gene expression patterns between the *Ciona* TSGs in  
190 the neural complex and their homologs in mice (left) or zebrafish (right) tissues were calculated.  
191 Mouse (62.5%) and zebrafish (48.2%) homologs of *Ciona* neural complex-specific genes  
192 showed high expression in the corresponding mouse and zebrafish brains. (B) Clustering of  
193 homologous genes in mice and zebrafish by tissue distribution. The heat map shows the  
194 expression levels of the homologs in the 30 mouse tissues (left) and 12 zebrafish tissues (right).  
195 The brain clusters are shown in orange. Gene symbols annotated with characteristic GO terms

196 for brain function and development and their *Ciona* homologous IDs are indicated in red. The  
197 red IDs in both mice and zebrafish are highlighted in yellow. (C) The neural complex-specific  
198 expression of the *Ciona* TSGs was confirmed by qRT-PCR (n=3-4). Expression is shown  
199 relative to the *Ciona* KDEL endoplasmic reticulum protein retention receptor 2 gene (*CiKdelr2*,  
200 KY.Chr10.704), which was found to be constitutively expressed among the 9 tissues, according  
201 to the RNA-seq analysis. P-values from statistical analyses with the Levene test, Kruskal-Wallis  
202 one-way ANOVA, and parametric one-way ANOVA are indicated as P<sub>L</sub>, P<sub>np</sub>, P<sub>p</sub>, respectively.  
203 AS, atrial siphon; Endo, endostyle; IntD, distal intestine; IntP, proximal intestine; IntM, middle  
204 intestine; NC, neural complex; OS, oral siphon; Ova, ovary; Pha, pharynx; Stom, stomach.

205

206 Vertebrate receptors for acetylcholine (*Chrn3*, *chrn3a*, *Chrm5*, and *chrm4a*) and GABA  
207 (*Gabra6* and *gabra4*) were also specifically expressed in the corresponding brain (Fig 3B),  
208 suggesting that fundamental functions of the neurotransmitters acetylcholine and GABA are  
209 conserved in chordates. With respect to the other neurotransmitter-related genes, 2 AMPA-type  
210 glutamate receptors (KY.Chr2.1128 and KY.Chr3.791) [28], 3 candidate metabotropic-type  
211 glutamate receptors (KY.Chr4.1146, KY.Chr12.932, KY.Chr6.541) [29], and 7 monoamine  
212 receptors (CiHT1-a, Ci5HT1-b, Ci5HT-2, Ci5HT7-a, CiADREβ-a, CiADREβ-b, and  
213 CiADREα-2a [30] were broadly expressed in several tissues (S1 Table). Moreover, most of the  
214 neuropeptide genes [14,15] showed high expression in the neural complex, but were also  
215 enriched in the siphons or other tissues (S1 Table). The peptide receptors [31] showed various  
216 tissue distributions (S1 Table). These results imply the strict functions of the cholinergic and  
217 GABAergic systems in the adult neural complex and broad functions of glutamate, monoamine,  
218 and neuropeptidergic systems in various tissues.

219 Interactions between immunoglobulin superfamily proteins, *Mdga* and the synaptic  
220 organizing protein *Nlgn*, are important for regulating the dynamic balance of synapse  
221 development in mice [32]. Specific expression of the zebrafish homologs (*mdga2a* and *nlgn3b*)  
222 and *Ciona* homologs (KY.Chr3.577 and KY.Chr7.428) suggest some conserved roles in synapse  
223 regulation. Of note, the expression of vertebrate homologs of the *Otp* gene was also restricted to  
224 the respective mouse and zebrafish brain (Fig 3B), suggesting that the essential roles of the  
225 homeobox protein in neurodevelopment is conserved in chordates. In contrast, a mouse  
226 homolog (*Six3*) of the other homeobox protein *Ciona Six3/6* (KY.Chr10.279) was exclusively  
227 expressed in the mouse brain; in contrast, the zebrafish homolog (*six3a*) was predominantly  
228 expressed in the zebrafish testis (Fig 3B), suggesting divergent roles of *Six3a* in zebrafish. None  
229 of the marker genes for specific neurons in *Ciona* embryos (e.g., *Dmbx* (KY.Chr1.2439) for  
230 decussating neurons and *Prop* for Eminens neurons) [7] showed tissue-specific expression in  
231 the adult tissues (S1 Table), suggesting multifunctionality of these genes or broad distribution



232 throughout the peripheral nervous systems.

233 Similar to the *Ciona* neural complex, 28.6% of mouse homologs of *Ciona* heart-specific  
234 genes were predominantly expressed in the mouse heart, and distinct sets of zebrafish homologs  
235 were expressed in the zebrafish heart (25.8%) and muscle (25.8%) (S2A Fig). Four mouse  
236 homologs essential for heart beating and development (*Mybpc3*, *Bmp10*, *Smyd1*, and *Mylk3*)  
237 were identified (S2B Fig and S2 Table) and specific expression of the *Ciona* homologs  
238 (KY.Chr1.628, KY.Chr14.1196, KY.Chr6.594, and KY.Chr3.1260) was confirmed (S2C Fig).  
239 BMP10 has been reported as a ligand for the ALK1 receptor and is important for vasculature  
240 development and maintenance in both zebrafish and mice [33]. Additionally, the  
241 myosin-interacting protein SMYD1 is essential for sarcomere organization in both species [34].  
242 Mutations in the myosin-binding protein C3 variant (*Mybpc3* and *mybpc3*) and myosin light  
243 chain kinase 3 (*Mylk3* and *mylk3*) cause hypertrophic and dilated cardiomyopathy in both  
244 species [35-37]. Accordingly, the essential genes for heart development are likely to be  
245 conserved in ascidians. Combined with the previous reports showing the transcriptomic  
246 similarities among the vertebrate brains and heart tissues [18,19], the current results suggest that  
247 the similarities in gene expression patterns in the brain or heart conform to not only vertebrates  
248 but also chordates including ascidians. Consequently, the fundamental functions of  
249 neurotransmission and heart beating, and organization of synapses and sarcomeres are likely to  
250 be conserved among ascidians, zebrafish, and mice.

251

## 252 **(ii) *Ciona*-unique gene-rich tissues: ovary, intestine, and** 253 **pharynx**

254 Surprisingly, expression profiles between *Ciona* TSGs and their homologs in the ovary and  
255 intestine were not similar to those in corresponding ovaries and intestines, but rather exhibited  
256 similarity to other tissues. Only 4.3% and 14.0% of the mouse and zebrafish homologs of *Ciona*  
257 ovary TSGs were highly expressed in the respective ovaries, whereas 30.4% and 14.0% were  
258 highly expressed in the mouse and zebrafish brain, respectively (S3A Fig). Similarly, 11.5% and  
259 13.5% of the mouse and zebrafish homologs of *Ciona* intestine TSGs were highly expressed in  
260 the respective intestines, while 44.2% and 15.4% were highly expressed in the zebrafish and  
261 mouse testis, respectively (S4A Fig). The pattern of TSG expression is likely indicative of the  
262 distinct reproductive and nutrient uptake processes among the species. In the ovary, 11 zebrafish  
263 homologs were included in the zebrafish ovary-rich cluster that were not found in mice (S3B  
264 Fig, pink). Thus, further studies of these genes are expected to be useful for understanding  
265 differences in the mechanisms of folliculogenesis and oogenesis between mammals and aquatic  
266 animals.

267 Other clusters of predominant expression with characteristic GO terms were observed in



268 several tissues (S3B Fig, *Ciona* IDs in red). Moreover, 8 genes were found in both mouse and  
269 zebrafish, but only one (KY.Chr7.498) shared a similar tissue distribution (high in the brain)  
270 (S3B Fig, highlighted in yellow). These results suggest that gene expression for female  
271 gametogenesis has diverged in a species-specific fashion. It is noteworthy that the current  
272 results are not inconsistent with our previous study demonstrating that the MAP kinase  
273 (*CiErk1/2*, KY.Chr6.139), maturation promoting factor (*CiCcnb*, KY.Chr4.1303 and *CiCdk1*,  
274 KY.UAContig35), and matrix metalloproteinase (*CiMmp2/9/13*, KY.Chr3.680), which play  
275 pivotal roles in the conserved pathway of oocyte maturation and ovulation [26], are  
276 multifunctional molecules that are widely distributed in various tissues, and are not specifically  
277 expressed in the ovary (S1 Table).

278 With respect to the intestine, the major cluster in zebrafish included *Ciona*-TSG homologs  
279 that were predominantly expressed in the testis, and 5 out of 19 genes harbored characteristic  
280 GO terms for meiosis (S4B Fig, pink and S2 Table). A moderate similarity to the mouse testis  
281 was also observed (S4A Fig), which may reflect a slight contamination of the invasive or  
282 adhesive testis to the *Ciona* intestine. The other 2 clusters of the brain and intestine were also  
283 found in both species (S4B Fig, orange), but functional annotations of most zebrafish genes  
284 were unavailable. Four common genes (S4B Fig, highlighted in yellow, KY.Chr3.158,  
285 KY.Chr8.667, KY.Chr14.625, and KY.Chr4.41) homologous to the mouse homeobox protein  
286 *Cdx*, intraflagellar transport protein, *Ttc*, DNA repair protein, *Rad51*, and beta-hexosaminidase,  
287 *Hexb*, showed specific expression in the *Ciona* intestine (S4C Fig). However, only the  
288 vertebrate *Cdx2* and *cdx4* genes were specifically expressed in the vertebrate intestine, while  
289 others were distributed among various tissues (S4B Fig), suggesting that the *Ciona* intestine  
290 might have evolved in a *Ciona*-specific manner.

291 The pharynx is responsible for respiration and food collection, as well as immune  
292 responses [11,38-40]. The current RNA-seq data confirmed the high expression of the  
293 immune-complement CiC3 gene (KY.Chr11.1089) and the CiTNF $\alpha$  gene (KY.Chr3.1442) (S1  
294 Table) reported in previous studies [38-40]. These findings are compatible with the view that  
295 the pharynx is an immune-responsive organ. However, comparative analysis of the zebrafish  
296 and mouse homologs was not performed, given that only 15 TSGs were newly identified, with  
297 12 having no homologous genes in zebrafish and mice (Fig 2). Thus, it is presumed that the  
298 pharynx might have evolved in a *Ciona*-specific lineage along with the development of  
299 *Ciona*-specific respiration, nutrient uptake, and immune systems.

300

### 301 **(iii) Homologous TSG-rich tissues histologically unrelated to** 302 **the vertebrate counterparts: siphons, endostyle, and stomach**

303 Of the TSGs in the siphons, 25.9% and 23.4% of the vertebrate homologs showed high

304 expression in the mouse and zebrafish brain, respectively (S5A Fig). Moreover, characteristic  
305 cluster and GO terms for brain function and development were observed (S5B Fig, orange, S2  
306 Table). These results are consistent with previous reports demonstrating that peptidergic  
307 neurons are enriched in the siphons and endostyle [12,13]. Additionally, 24.1%, 23.4%, and  
308 21.9% of the vertebrate homologs were highly expressed in the mouse limb of E14.5 embryo,  
309 zebrafish embryo, and zebrafish intestine, respectively (S5 Fig), raising the possibility that  
310 siphons retain a group of genes expressed during embryogenesis or have an ancestral function in  
311 the intestinal system. Although 6 genes were found as common in mice and zebrafish, only 1  
312 gene (KY.Chr14.962) exhibited orthologous hits from the BLATP analysis of mice and  
313 zebrafish (collagen type XII, *Coll2a1* and *coll2a1a*) and the other 5 genes resulted in different  
314 BLAST hits between mice and zebrafish (S5B Fig, highlighted in yellow). Combined with the  
315 fact that definite siphon counterparts in the mouse and zebrafish tissues are unclear, these results  
316 suggest that siphon-specific genes and their homologs might have evolved in a species-specific  
317 lineage with divergent roles in each tissue.

318 Similar results were observed in the TSGs in endostyle; 28.6% and 18.5% of the vertebrate  
319 homologs showed high expression in the mouse and zebrafish brain, respectively (S6A Fig)  
320 with a characteristic cluster and GO terms for brain function and development (S6B Fig, orange,  
321 S2 Table). One homolog (KY.Chr6.400) of the *Slit* gene, which is important for neural  
322 development, was specifically expressed in the endostyle (S6C Fig). The endostyle is believed  
323 to share some functions with the vertebrate thyroid gland by the prominent expression of the  
324 thyroid-related genes and roles in regulating iodine concentrations [41-44]. The current study  
325 confirmed the previous endostyle-specific expression of the *CiVWFL* genes (KY.Chr1.1785 and  
326 KY.Chr10.1161) [45] and predominant expression of the thyroid-related transcription factor  
327 genes (*Foxe*, KY.Chr5.63 and *Foxq*, KY.Chr3.324) [41] (S1 Table). The *Ciona* galectins  
328 (*CiLgals*, KY.Chr4.949 and KY.Chr6.43), the immune-responsive genes expressed in the  
329 endostyle [46], were found to be expressed not only in the endostyle but also in the neural  
330 complex, pharynx, stomach, intestine and the other tissues (S1 Table). Collectively, the present  
331 data support the previous study demonstrating that the endostyle is a thyroid-related organ.

332 Intriguingly, only 4.8% of the mouse homologs of the *Ciona* stomach-specific genes were  
333 highly expressed in the mouse stomach, whereas 28.6% and 33.3% were expressed in the mouse  
334 liver and intestine, respectively. Similarly, 34.8%, 21.7%, and 17.4% of the zebrafish homologs  
335 were highly expressed in the zebrafish kidney, intestine, and liver, respectively (Fig 4A). The  
336 mouse homologs of *Ciona* TSGs in the stomach showed 2 major clusters of highly expressed  
337 genes in the intestine and liver with the characteristic GO terms for these tissues (Fig 4B,  
338 orange, *Ciona* IDs in red, and S2 Table). Likewise, zebrafish homologs showed 3 clusters in the  
339 intestine, liver, and kidney with the characteristic GO terms for these tissues (Fig 4B, orange,

340 *Ciona* IDs in red, and S2 Table). Moreover, 6 homologs (carboxypeptidase A, *Cpa2*,  
341 cytochrome P450, *Cyp2*, interferon regulatory factor, *Irf*, and 3 fibrinogen-related genes, *Fgg*,  
342 *Fgb*, or *Fcna*) of the *Ciona* TSGs (KY.Chr8.1333, KY.Chr11.806, KY.Chr14.909,  
343 KY.Chr14.910, KY.Chr14.911, and KY.Chr14.393) were found in both mice and zebrafish (Fig  
344 4B, highlighted in yellow) and tissue specificities of the *Ciona* TSGs were confirmed by  
345 qRT-PCR (Fig 4C). Therefore, the *Ciona* stomach may play various roles (such as metabolism  
346 of protein and low molecular weight compounds, inflammatory responses, and/or blood  
347 regulation) similar to the vertebrate intestine, kidney, and liver. It is also noteworthy that the  
348 major pancreatic digestive enzymes (alpha-amylase (KY.Chr5.116), lipase (KY.Chr7.356),  
349 trypsin (KY.Chr4.1293), chymotrypsin (KY.Chr10.63), and carboxypeptidase  
350 (KY.Chr12.113)), which were previously shown to be specifically expressed in the juvenile  
351 stomach [47], were highly expressed in the adult stomach as well as in the distal region of the  
352 intestine (S1 Table). These findings suggest distinct roles (or substrates) of these enzymes in the  
353 distal region of the intestine from the juvenile and/or adult stomach. Combined with the fact that  
354 no orthologs for gastric digestive enzymes, such as pepsin or carboxypeptidase E, were found in  
355 the *Ciona* genome, the current results support the hypothesis that the *Ciona* stomach may not be  
356 a simple structural and functional homolog of the vertebrate stomach [47,48]. In other words,  
357 the *Ciona* stomach might not only function as a “stomach” but also, at least in part, share some  
358 features of the pancreas, liver, kidney, and intestine of vertebrates.

359

360 **Fig 4. Comparative analyses of *Ciona* TSGs in the stomach and their homologs in mouse**  
361 **and zebrafish.** (A) Similarities in gene expression patterns between the *Ciona* TSGs in the  
362 stomach and their homologs in mouse (left) or zebrafish (right) tissues were calculated as in Fig  
363 3A. Approximately 30% of the homologous genes were highly expressed in the mouse liver and  
364 intestine, while 20-35% were highly expressed in the zebrafish liver, kidney, and intestine. (B)  
365 Clustering by tissue distribution of the homologous genes in mice and zebrafish. The heat maps  
366 are shown as in Fig 3B. Clusters of highly expressed genes in the mouse brain, intestine,  
367 zebrafish kidney, liver, and intestine are shown in orange. (C) Stomach-specific expression of  
368 *Ciona* TSGs in the stomach was confirmed by qRT-PCR (n=3-4). Data are presented as in Fig  
369 3C.

370

## 371 **Evolutionary aspects of each tissue in chordates**

372 Tissue similarities based on the comparative analyses of transcriptomic profiles among the  
373 species were investigated in this study. The *Ciona* neural complex and heart were highly similar  
374 to the corresponding counterparts in vertebrates (Fig 5A and B) in that gene expression patterns  
375 for the *Ciona* TSGs and their homologs (e.g., *Chrn3*, *Otp*, *Mybpc3*, and *Bmp10*, etc.) suggested

376 conserved organization of synapses and sarcomeres, and consequent similarity in their  
377 biological roles in neurotransmission and heart beating (Figs 3 and S2). *Ciona* intestine and  
378 ovary were not similar to the corresponding vertebrate tissues, but did exhibit similarity to  
379 several other vertebrate tissues, implying a divergence of reproductive strategies and/or nutrient  
380 uptakes (S3 and S4 Figs). *Ciona* pharynx might have evolved in a *Ciona*-specific lineage, given  
381 that most TSGs in the pharynx were *Ciona*-specific (Fig 2). The *Ciona* stomach was more  
382 similar to the vertebrate liver, kidney, and intestine rather than the mouse stomach (Fig 5C).  
383 Given that *Ciona* homologs of mouse *Cpa2*, *Cyp2*, *Irf*, and fibrinogen-related genes were  
384 specifically expressed in the *Ciona* stomach, the *Ciona* stomach might have evolved to play  
385 various roles normally attributed to the vertebrate liver, kidney, and intestine, such as  
386 metabolism of organic compounds and inflammatory responses (Fig 4).

387

388 **Fig 5. Schematic summary of the comparative analyses of the brain, heart, and stomach.**

389 Similarities in gene expression patterns between the *Ciona* and zebrafish or mouse tissues  
390 illustrated using Cytoscape software (ver. 3.8.2.). *Ciona*, zebrafish, and mouse tissues are shown  
391 as pink, green, and blue nodes, respectively. The width of the lines represents the similarity  
392 between the tissues. (A) The *Ciona* neural complex and several other tissues showed high  
393 similarities to the zebrafish and mouse brain. (B) The *Ciona* heart was similar to the  
394 corresponding heart and muscle of vertebrates. (C) The *Ciona* stomach was not similar to the  
395 mouse stomach, but rather was similar to several other tissues including the liver, kidney, and  
396 intestine.

397

398 Of particular interest is that several *Ciona* tissues showed high or moderate similarities to  
399 the vertebrate brain in light of TSG expression (Fig 5A). This indicates that some *Ciona*  
400 homologs of the highly expressed genes in the vertebrate brain might have diverged as  
401 peripheral tissue-specific genes in ascidians. In the case of the *Ciona* ovary, 28 vertebrate  
402 homologs of the *Ciona* TSGs were specifically expressed in the mouse and zebrafish brain, but  
403 most of these were not annotated with characteristic GO terms for brain function or  
404 development (S2 Table), suggesting that these genes have evolved a functionally distinct  
405 lineage. However, 22 vertebrate homologs of the *Ciona* TSGs in the siphons were highly  
406 expressed in the vertebrate brain and 10 of these were annotated with characteristic GO terms  
407 for brain function and development (e.g., CNS development [GO:0007417] for *Bcan*, synapse  
408 organization [GO:0050808] for *Adgrl2*, and axon extension [GO:0048675] for *sema5a*, etc.) (S2  
409 Table). Such vertebrate homologs harboring GO terms for brain development and function were  
410 found in *Ciona* TSGs of the endostyle (e.g., axonogenesis [GO:0007409] for *Slit1*, etc.) and  
411 intestine (e.g., dorsal spinal cord development [GO:0021516] for *Uncx*, etc.) (S2 Table). These

412 results suggest that direct or local regulation of peripheral tissues by the peripheral nervous  
413 system is more dominant in ascidians than in vertebrates. Such a view is in good agreement with  
414 our findings that the *Ciona* siphons and endostyle were similar to the vertebrate brain (S5 and  
415 S6 Figs) and also with a previous study revealing that *Ciona* peripheral tissues are regulated by  
416 direct projections of the peripheral nervous system [12,13]. Collectively, while vertebrates  
417 might have evolved complicated regulatory systems by the acquisition of a sophisticated brain  
418 organ and indirect regulation via the circulatory system of closed vasculature, ascidians might  
419 have evolved a simple regulatory system represented by direct or local regulation by the  
420 peripheral nervous system or by a simple circulatory system of open vasculature.

421 In conclusion, we have obtained the transcriptomic profiles and identified TSGs for the  
422 adult tissues of an ascidian, *C. intestinalis* Type A (or *C. robusta*), which lies in a critical  
423 position on the phylogenetic tree of chordates. We have also evaluated the tissue similarities  
424 between ascidians and zebrafish or mice based on the tissue distribution of *Ciona* TSGs and  
425 their homologs in vertebrates. The current study provides important insights into the  
426 evolutionary lineages of function and development of tissues in chordates, and will pave the  
427 way for understanding the conservation and diversification of animal tissues among these  
428 species.

429  
430

## 431 **Materials and Methods**

### 432 **RNA extraction, purification, and RNA-seq analyses**

433 Adult ascidians were excised and 9 tissues (oral siphon, atrial siphon, neural complex,  
434 endostyle, heart, ovary, pharynx, stomach, and intestine) were collected from more than 4  
435 individuals. The intestine was divided into 3 parts (proximal, middle, and distal). Total RNA  
436 was extracted, purified, and treated with DNase as previously described [26]. A total of 500 ng  
437 of quality-confirmed RNA was subjected to RNA-seq using a HiSeq1500 (Illumina, San Diego,  
438 CA) in rapid mode, as previously described [26]. The resultant reads were aligned to the KY  
439 gene model of the *Ciona* cDNA library [3], which was downloaded from the ghost database  
440 ([http://ghost.zool.kyoto-u.ac.jp/default\\_ht.html](http://ghost.zool.kyoto-u.ac.jp/default_ht.html)). The expression level for each gene was  
441 calculated as gene-specific RPKM. TSGs were determined by exclusive gene expression:  
442 RPKM > 1 in a particular tissue and RPKM < 0.5 in all other tissues. TSGs for the siphons and  
443 intestine include the genes with RPKM > 1 either in the oral siphon or atrial siphon and in any  
444 part of the intestine, respectively. Total reads, mapping rates, accession numbers, and number of  
445 TSGs are summarized in Table 1. Raw reads and calculated RPKM for each gene are listed in  
446 Table S1. The raw sequence data have been deposited in the NCBI database (PRJNA731286).



447

## 448 **RNA-seq data analysis**

449 Amino acid sequences for the *Ciona* TSGs were obtained from the ghost database  
450 ([http://ghost.zool.kyoto-u.ac.jp/default\\_ht.html](http://ghost.zool.kyoto-u.ac.jp/default_ht.html)). BLASTP was run against the RefSeq protein  
451 database of mouse and zebrafish genes, which were downloaded from the NCBI FTP site  
452 (<https://ftp.ncbi.nlm.nih.gov/>). The threshold was set to an e-value of  $< 1e-5$ . The resultant  
453 BLASTP hits were considered as mouse or zebrafish genes homologous to *Ciona* TSGs, while  
454 the *Ciona* genes lacking hits in BLASTP were considered *Ciona* specific. The tissue distribution  
455 for the mouse or zebrafish homologs was investigated using public data. RNA-seq data for 30  
456 mouse tissues (PRJNA267840) and 12 zebrafish tissues (PRJNA255848) were used. Processed  
457 data for mouse gene expression with RefSeqID were directly downloaded from NCBI.  
458 Zebrafish data were downloaded from the PhyloFish Portal  
459 (<http://phylofish.sigenae.org/index.html>) and the contigIDs were converted to RefSeqID via  
460 BLASTN and BioDBnet (<https://biodbnet-abcc.ncifcrf.gov/>). Expression levels for the mouse or  
461 zebrafish homologs of *Ciona* TSGs were normalized from 0 (as in a tissue with the lowest  
462 expression level) to 1 (as in a tissue with the highest expression level). The number of highly  
463 expressed genes ( $> 0.8$ ) in each tissue was counted and the ratio was indicated as “tissue  
464 similarity” between *Ciona* and zebrafish or mice. Gene ontology for highly expressed genes of  
465 mouse or zebrafish homologs was investigated in uniprot (<https://www.uniprot.org/>). Clustering  
466 by tissue distribution was performed using R software (ver. 4.0.0, <https://www.r-project.org/>).

467

## 468 **qRT-PCR**

469 RNA-seq data was confirmed by qRT-PCR using another 3-4 sets of *Ciona* tissues. The  
470 qRT-PCR was performed as previously described [26]. In brief, an aliquot of 1  $\mu$ g of  
471 DNase-treated total RNA isolated from *Ciona* tissues was used for the first-strand cDNA  
472 synthesis. qRT-PCR was performed using a CFX96 Real-time System and SsoAdvanced™  
473 Universal SYBR Green Supermix (Bio-Rad laboratories, Hercules, CA). The primers are listed  
474 in Table S3. Gene expression levels were normalized to the *Ciona* KDEL endoplasmic  
475 reticulum protein retention receptor 2 (*CiKdelr2*, KY.Chr10.704), which was found to be  
476 constitutively expressed among 9 tissues according to the RNA-seq analysis.

477

## 478 **Statistical analysis**

479 dCt values for the qRT-PCR of the *Ciona* tissues were used for statistical analyses, as  
480 reported elsewhere [49,50]. The expression level was set to 0 for genes that were not detected,  
481 and samples with 2 or more sets below detection were excluded from the statistical analysis.  
482 Statistical analyses were performed using R software. We first analyzed using the Levene test

483 and examined the homoscedasticity of each group (tissue). Genes that exhibited equal variances  
484 among the tissues were analyzed by a parametric one-way analysis of variance (ANOVA),  
485 followed by the Tukey *post hoc* test. Genes that did not show equal variances were analyzed  
486 using a nonparametric Kruskal-Wallis one-way ANOVA, followed by the Dunnett test and  
487 Bonferroni adjustment. Differences were considered statistically significant at  $P < 0.05$ .  
488 P-values for the Levene test, Kruskal-Wallis one-way ANOVA, and parametric one-way  
489 ANOVA are indicated as  $P_L$ ,  $P_{np}$ ,  $P_p$ , respectively. P-values for the *post hoc* multiple tests are  
490 shown in the S1 File.

491

492

## 493 **Acknowledgments**

494 We acknowledge the National Bio-Resource Project for providing ascidians. We are also  
495 grateful to Prof. Shigetada Nakanishi for providing fruitful comments regarding the manuscript.  
496 This work was supported in part by grants from the Japan Society for the Promotion of Science  
497 to SM (JP19K16182).

498

499

## 500 **References**

- 501 1. Delsuc F, Brinkmann H, Chourrout D, Philippe H. Tunicates and not cephalochordates  
502 are the closest living relatives of vertebrates. *Nature*. 2006;439: 965-968. DOI:  
503 10.1038/nature04336 PMID: 16495997
- 504 2. Satoh N, Rokhsar D, Nishikawa T. Chordate evolution and the three-phylum system. *Proc*  
505 *Biol Sci*. 2014; 281: 20141729. DOI: 10.1098/rspb.2014.1729 PMID: 25232138 PMCID:  
506 PMC4211455
- 507 3. Satou Y, Nakamura R, Yu D, Yoshida R, Hamada M, Fujie M et al. A Nearly Complete  
508 Genome of *Ciona intestinalis* Type A (*C. robusta*) Reveals the Contribution of Inversion  
509 to Chromosomal Evolution in the Genus *Ciona*. *Genome Biol Evol*. 2019; 11: 3144-3157.  
510 DOI: 10.1093/gbe/evz228 PMID: 31621849 PMCID: PMC6836712
- 511 4. Liu B, Satou Y. The genetic program to specify ectodermal cells in ascidian embryos.  
512 *Dev Growth Differ*. 2020; 62: 301-310. DOI: 10.1111/dgd.12660 PMID: 32130723
- 513 5. Lemaire P. Evolutionary crossroads in developmental biology: the tunicates.  
514 *Development*. 2011; 138: 2143-2152. DOI: 10.1242/dev.048975 PMID: 21558365
- 515 6. Satoh N. The ascidian tadpole larva: comparative molecular development and genomics.  
516 *Nat Rev Genet*. 2003; 4: 285-295. DOI: 10.1038/nrg1042 PMID: 12671659



- 517 7. Cao C, Lemaire LA, Wang W, Yoon PH, Choi YA, Parsons LR et al. Comprehensive  
518 single-cell transcriptome lineages of a proto-vertebrate. *Nature*. 2019; 571: 349-354. DOI:  
519 10.1038/s41586-019-1385-y PMID: 31292549 PMCID: PMC6978789
- 520 8. Horie R, Hazbun A, Chen K, Cao C, Levine M, Horie T. Shared evolutionary origin of  
521 vertebrate neural crest and cranial placodes. *Nature*. 2018; 560: 228-232. DOI:  
522 10.1038/s41586-018-0385-7 PMID: 30069052 PMCID: PMC6390964
- 523 9. Nishida H. Cell lineage analysis in ascidian embryos by intracellular injection of a tracer  
524 enzyme. III. Up to the tissue restricted stage. *Dev Biol*. 1987; 121: 526-541. DOI:  
525 10.1016/0012-1606(87)90188-6 PMID: 3582738
- 526 10. Chiba S, Sasaki A, Nakayama A, Takamura K, Satoh N. Development of *Ciona*  
527 *intestinalis* juveniles (through 2nd ascidian stage). *Zoolog Sci*. 2004; 21: 285-298. DOI:  
528 10.2108/zsj.21.285 PMID: 15056923
- 529 11. Goodbody I. The physiology of ascidians. *Adv Mar Biol*. 1974; 12: 1-149.
- 530 12. Osugi T, Sasakura Y, Satake H. The ventral peptidergic system of the adult ascidian  
531 *Ciona robusta* (*Ciona intestinalis* Type A) insights from a transgenic animal model. *Sci*  
532 *Rep*. 2020; 10: 1892. DOI: 10.1038/s41598-020-58884-w PMID: 32024913 PMCID:  
533 PMC7002689
- 534 13. Osugi T, Sasakura Y, Satake H. The nervous system of the adult ascidian *Ciona*  
535 *intestinalis* Type A (*Ciona robusta*): Insights from transgenic animal models. *PLoS One*.  
536 2017; 12: e0180227. DOI: 10.1371/journal.pone.0180227 PMID: 28651020 PMCID:  
537 PMC5484526
- 538 14. Matsubara S, Kawada T, Sakai T, Aoyama M, Osugi T, Shiraishi A et al. The  
539 significance of *Ciona intestinalis* as a stem organism in integrative studies of functional  
540 evolution of the chordate endocrine, neuroendocrine, and nervous systems. *Gen Comp*  
541 *Endocrinol*. 2016; 227: DOI: 10.1016/j.ygcen.2015.05.010 101-108. PMID: 26031189
- 542 15. Kawada T, Ogasawara M, Sekiguchi T, Aoyama M, Hotta K, Oka K et al. Peptidomic  
543 analysis of the central nervous system of the protochordate, *Ciona intestinalis*: homologs  
544 and prototypes of vertebrate peptides and novel peptides. *Endocrinology*. 2011; 152:  
545 2416-2427. DOI: 10.1210/en.2010-1348 PMID: 21467196
- 546 16. Breschi A, Djebali S, Gillis J, Pervouchine DD, Dobin A, Davis CA et al. Gene-specific  
547 patterns of expression variation across organs and species. *Genome Biol*. 2016; 17: 151.  
548 DOI: 10.1186/s13059-016-1008-y PMID: 27391956 PMCID: PMC4937605
- 549 17. Sudmant PH, Alexis MS, Burge CB. Meta-analysis of RNA-seq expression data across  
550 species, tissues and studies. *Genome Biol*. 2015; 16: 287. DOI:  
551 10.1186/s13059-015-0853-4 PMID: 26694591 PMCID: PMC4699362
- 552 18. Merkin J, Russell C, Chen P, Burge CB. Evolutionary dynamics of gene and isoform

- 553 regulation in Mammalian tissues. *Science*. 2012; 338: 1593-1599. DOI:  
554 10.1126/science.1228186 PMID: 23258891 PMCID: PMC3568499
- 555 19. Brawand D, Soumillon M, Necsulea A, Julien P, Csardi G, Harrigan P et al. The  
556 evolution of gene expression levels in mammalian organs. *Nature*. 2011; 478: 343-348.  
557 DOI: 10.1038/nature10532 PMID: 22012392
- 558 20. Kryuchkova-Mostacci N, Robinson-Rechavi M. Tissue-Specificity of Gene Expression  
559 Diverges Slowly between Orthologs, and Rapidly between Paralogs. *PLoS Comput Biol*.  
560 2016; 12: e1005274. DOI: 10.1371/journal.pcbi.1005274 PMID: 28030541 PMCID:  
561 PMC5193323
- 562 21. Altenhoff AM, Studer RA, Robinson-Rechavi M, Dessimoz C. Resolving the ortholog  
563 conjecture: orthologs tend to be weakly, but significantly, more similar in function than  
564 paralogs. *PLoS Comput Biol*. 2012; 8: e1002514. DOI: 10.1371/journal.pcbi.1002514  
565 PMID: 22615551 PMCID: PMC3355068
- 566 22. Imai KS, Hino K, Yagi K, Satoh N, Satou Y. Gene expression profiles of transcription  
567 factors and signaling molecules in the ascidian embryo: towards a comprehensive  
568 understanding of gene networks. *Development*. 2004; 131: 4047-4058. DOI:  
569 10.1242/dev.01270 PMID: 15269171
- 570 23. Satou Y, Yamada L, Mochizuki Y, Takatori N, Kawashima T, Sasaki A et al. A cDNA  
571 resource from the basal chordate *Ciona intestinalis*. *Genesis*. 2002; 33: 153-154. DOI:  
572 10.1002/gene.10119 PMID: 12203911
- 573 24. Ogasawara M, Sasaki A, Metoki H, Shin-i T, Kohara Y, Satoh N et al. Gene expression  
574 profiles in young adult *Ciona intestinalis*. *Dev Genes Evol*. 2002; 212: 173-185. DOI:  
575 10.1007/s00427-002-0230-7 PMID: 12012232
- 576 25. Kawada T, Shiraishi A, Aoyama M, Satake H. Transcriptomes of the Premature and  
577 Mature Ovaries of an Ascidian, *Ciona intestinalis*. *Front Endocrinol (Lausanne)*. 2017; 8:  
578 88. DOI: 10.3389/fendo.2017.00088 PMID: 28484427 PMCID: PMC5402223
- 579 26. Matsubara S, Shiraishi A, Osugi T, Kawada T, Satake H. The regulation of oocyte  
580 maturation and ovulation in the closest sister group of vertebrates. *Elife*. 2019; 8: e49062.  
581 DOI: 10.7554/eLife.49062 PMID: 31573508 PMCID: PMC6786877
- 582 27. Shoguchi E, Hamada M, Fujie M, Satoh N. Direct examination of chromosomal  
583 clustering of organ-specific genes in the chordate *Ciona intestinalis*. *Genesis*. 2011; 49:  
584 662-672. DOI: 10.1002/dvg.20730 PMID: 21328518
- 585 28. Hirai S, Hotta K, Kubo Y, Nishino A, Okabe S, Okamura Y et al. AMPA glutamate  
586 receptors are required for sensory-organ formation and morphogenesis in the basal  
587 chordate. *Proc Natl Acad Sci U S A*. 2017; 114: 3939-3944. DOI:  
588 10.1073/pnas.1612943114 PMID: 28348228 PMCID: PMC5393200

- 589 29. Kamesh N, Aradhyam GK, Manoj N. The repertoire of G protein-coupled receptors in the  
590 sea squirt *Ciona intestinalis*. BMC Evol Biol. 2008; 8: 129. DOI:  
591 10.1186/1471-2148-8-129 PMID: 18452600 PMCID: PMC2396169
- 592 30. Razy-Krajka F, Brown ER, Horie T, Callebert J, Sasakura Y, Joly JS et al.  
593 Monoaminergic modulation of photoreception in ascidian: evidence for a  
594 proto-hypothalamo-retinal territory. BMC Biol. 2012; 10: 45. DOI:  
595 10.1186/1741-7007-10-45 PMID: 22642675 PMCID: PMC3414799
- 596 31. Shiraishi A, Okuda T, Miyasaka N, Osugi T, Okuno Y, Inoue J et al. Repertoires of G  
597 protein-coupled receptors for *Ciona*-specific neuropeptides. Proc Natl Acad Sci U S A.  
598 2019; 116: 7847-7856. DOI: 10.1073/pnas.1816640116 PMID: 30936317 PMCID:  
599 PMC6475428
- 600 32. Connor SA, Elegheert J, Xie Y, Craig AM. Pumping the brakes: suppression of synapse  
601 development by MDGA-neurologin interactions. Curr Opin Neurobiol. 2019; 57: 71-80.  
602 DOI: 10.1016/j.conb.2019.01.002 PMID: 30771697
- 603 33. Capasso TL, Li B, Volek HJ, Khalid W, Rochon ER, Anbalagan A et al.  
604 BMP10-mediated ALK1 signaling is continuously required for vascular development and  
605 maintenance. Angiogenesis. 2020; 23: 203-220. DOI: 10.1007/s10456-019-09701-0  
606 PMID: 31828546 PMCID: PMC7165044
- 607 34. Just S, Meder B, Berger IM, Etard C, Trano N, Patzel E et al. The myosin-interacting  
608 protein SMYD1 is essential for sarcomere organization. J Cell Sci. 2011; 124: 3127-3136.  
609 DOI: 10.1242/jcs.084772 PMID: 21852424
- 610 35. Da'as SI, Yalcin HC, Nasrallah GK, Mohamed IA, Nomikos M, Yacoub MH et al.  
611 Functional characterization of human myosin-binding protein C3 variants associated with  
612 hypertrophic cardiomyopathy reveals exon-specific cardiac phenotypes in zebrafish  
613 model. J Cell Physiol. 2020; 235: 7870-7888. DOI: 10.1002/jcp.29441 PMID: 31943169
- 614 36. Giles J, Patel JR, Miller A, Iverson E, Fitzsimons D, Moss RL. Recovery of left  
615 ventricular function following in vivo reexpression of cardiac myosin binding protein C. J  
616 Gen Physiol. 2019; 151: 77-89. DOI: 10.1085/jgp.201812238 PMID: 30573635 PMCID:  
617 PMC6314388
- 618 37. Tobita T, Nomura S, Morita H, Ko T, Fujita T, Toko H et al. Identification of MYLK3  
619 mutations in familial dilated cardiomyopathy. Sci Rep. 2017; 7: 17495. DOI:  
620 10.1038/s41598-017-17769-1 PMID: 29235529 PMCID: PMC5727479
- 621 38. Giacomelli S, Melillo D, Lambris JD, Pinto MR. Immune competence of the *Ciona*  
622 *intestinalis* pharynx: complement system-mediated activity. Fish Shellfish Immunol.  
623 2012; 33: 946-952. DOI: 10.1016/j.fsi.2012.08.003 PMID: 22967954
- 624 39. Parrinello N, Vizzini A, Arizza V, Salerno G, Parrinello D, Cammarata M et al. Enhanced

- 625 expression of a cloned and sequenced *Ciona intestinalis* TNFalpha-like (CiTNF alpha)  
626 gene during the LPS-induced inflammatory response. Cell Tissue Res. 2008; 334:  
627 305-317. DOI: 10.1007/s00441-008-0695-4 PMID: 18936978
- 628 40. Parrinello N, Vizzini A, Salerno G, Sanfratello MA, Cammarata M, Arizza V et al.  
629 Inflamed adult pharynx tissues and swimming larva of *Ciona intestinalis* share  
630 CiTNFalpha-producing cells. Cell Tissue Res. 2010; 341: 299-311. DOI:  
631 10.1007/s00441-010-0993-5 PMID: 20563600
- 632 41. Ogasawara M, Satou Y. Expression of FoxE and FoxQ genes in the endostyle of *Ciona*  
633 *intestinalis*. Dev Genes Evol. 2003; 213: 416-419. DOI: 10.1007/s00427-003-0342-8  
634 PMID: 12802588
- 635 42. Ogasawara M. Overlapping expression of amphioxus homologs of the thyroid  
636 transcription factor-1 gene and thyroid peroxidase gene in the endostyle: insight into  
637 evolution of the thyroid gland. Dev Genes Evol. 2000; 210: 231-242. DOI:  
638 10.1007/s004270050309 PMID: 11180827
- 639 43. Ogasawara M, Di Lauro R, Satoh N. Ascidian homologs of mammalian thyroid  
640 peroxidase genes are expressed in the thyroid-equivalent region of the endostyle. J Exp  
641 Zool. 1999; 285: 158-169. DOI:  
642 10.1002/(sici)1097-010x(19990815)285:2<158::aid-jez8>3.0.co;2-0 PMID: 10440727
- 643 44. Ogasawara M, Di Lauro R, Satoh N. Ascidian homologs of mammalian thyroid  
644 transcription factor-1 gene are expressed in the endostyle. Zoolog Sci. 1999; 16: 559-565.  
645 DOI: <https://doi.org/10.2108/zsj.16.559>
- 646 45. Sasaki A, Miyamoto Y, Satou Y, Satoh N, Ogasawara M. Novel endostyle-specific genes  
647 in the ascidian *Ciona intestinalis*. Zoolog Sci. 2003; 20: 1025-1030. DOI:  
648 10.2108/zsj.20.1025 PMID: 12951410
- 649 46. Parrinello D, Sanfratello MA, Vizzini A, Parrinello N, Cammarata M. *Ciona intestinalis*  
650 galectin (CiLgals-a and CiLgals-b) genes are differentially expressed in endostyle zones  
651 and challenged by LPS. Fish Shellfish Immunol. 2015; 42: 171-176. DOI:  
652 10.1016/j.fsi.2014.10.026 PMID: 25449708
- 653 47. Nakayama S, Ogasawara M. Compartmentalized expression patterns of pancreatic- and  
654 gastric-related genes in the alimentary canal of the ascidian *Ciona intestinalis*:  
655 evolutionary insights into the functional regionality of the gastrointestinal tract in  
656 Olfactores. Cell Tissue Res. 2017; 370: 113-128. DOI: 10.1007/s00441-017-2627-7  
657 PMID: 28547657
- 658 48. Nakayama S, Sekiguchi T, Ogasawara M. Molecular and evolutionary aspects of the  
659 protochordate digestive system. Cell Tissue Res. 2019; 377: 309-320. DOI:  
660 10.1007/s00441-019-03035-5 PMID: 31049686

- 661 49. Ganger MT, Dietz GD, Ewing SJ. A common base method for analysis of qPCR data and  
662 the application of simple blocking in qPCR experiments. BMC Bioinformatics. 2017; 18:  
663 534. DOI: 10.1186/s12859-017-1949-5 PMID: 29191175 PMCID: PMC5709943
- 664 50. Yuan JS, Reed A, Chen F, Stewart CN Jr. Statistical analysis of real-time PCR data. BMC  
665 Bioinformatics. 2006; 7: 85. DOI: 10.1186/1471-2105-7-85 PMID: 16504059 PMCID:  
666 PMC1395339
- 667  
668

## 669 **Supporting information**

670 **S1 Fig. Validation of the RNA-seq data by referring to previously identified TSGs.** The  
671 tissue specificity of the TSGs previously reported by Shoguchi et al., 2011 [27] was confirmed  
672 in the current RNA-seq data. AS, atrial siphon; Endo, endostyle; IntD, distal intestine; IntP,  
673 proximal intestine; IntM, middle intestine; NC, neural complex; OS, oral siphon; Ova, ovary;  
674 Pha, pharynx; Stom, stomach.

675

676 **S2 Fig. Comparative analyses of *Ciona* TSGs in the heart and their homologs in mouse  
677 and zebrafish.** (A) Similarities between *Ciona* heart and mouse (left) or zebrafish (right) tissues  
678 were calculated as in Fig 3A. Approximately 30% and 25% of the homologous genes were  
679 highly expressed in the mouse heart and zebrafish heart and muscle, respectively. (B) Clustering  
680 by tissue distribution of the homologous genes in mice and zebrafish. The heat maps are shown  
681 as in Fig 3B. (C) The heart-specific expression of *Ciona* TSGs was confirmed by qRT-PCR  
682 (n=3-4). Data are presented as in Fig 3C.

683

684 **S3 Fig. Comparative analyses of *Ciona* TSGs in the ovary and their homologs in mouse  
685 and zebrafish.** (A) Similarities between *Ciona* ovary and mouse (left) or zebrafish (right)  
686 tissues were calculated as in Fig 3A. (B) Clustering by tissue distribution of the homologous  
687 genes in mice and zebrafish. The heat maps are shown as in Fig 3B. The zebrafish-ovary cluster  
688 is shown in pink.

689

690 **S4 Fig. Comparative analyses of *Ciona* TSGs in the intestine and their homologs in mouse  
691 and zebrafish.** (A) Similarities between *Ciona* intestine and mouse (left) or zebrafish (right)  
692 tissues were calculated as in Fig 3A. (B) Clustering by tissue distribution of the homologous  
693 genes in mice and zebrafish. The heat maps are shown as in Fig 3B. The clusters of highly  
694 expressed genes in the mouse brain and intestine are shown in orange, and that of the zebrafish  
695 testis is shown in pink. (C) The intestine-specific expression of *Ciona* TSGs in the heart were

696 confirmed by qRT-PCR (n=3-4). Data are presented as in Fig 3C.

697

698 **S5 Fig. Comparative analyses of *Ciona* TSGs in the siphons and their homologs in mouse**

699 **and zebrafish.** (A) Similarities between *Ciona* siphons and mouse (left) or zebrafish (right)

700 tissues were calculated as in Fig 3A. (B) Clustering by tissue distribution of the homologous

701 genes in mice and zebrafish. The heat maps are shown as in Fig 3B. The clusters of highly

702 expressed genes in the vertebrate brain are shown in orange.

703

704 **S6 Fig. Comparative analyses of *Ciona* TSGs in the endostyle and their homologs in mouse**

705 **and zebrafish.** (A) Similarities between *Ciona* endostyle and mouse (left) or zebrafish (right)

706 tissues were calculated as in Fig 3A. (B) Clustering by tissue distribution of the homologous

707 genes in mice and zebrafish. The heat maps are shown as in Fig 3B. The clusters of highly

708 expressed genes in the vertebrate brain are shown in orange. (C) The endostyle-specific

709 expression of *Ciona* TSGs in the endostyle was confirmed by qRT-PCR (n=3-4). Data are

710 presented as in Fig 3C.

711

712 **S1 Table. Raw reads and calculated RPKM values for RNA-seq data.**

713

714 **S2 Table. *Ciona* TSGs with GO terms.**

715

716 **S3 Table. Primers used in this study.**

717

718 **S1 File. Summary of statistical analysis results.** Differences were considered statistically

719 significant at  $P < 0.05$  (\*,  $P < 0.05$ ; \*\*,  $P < 0.01$ ).



# Figure 1

bioRxiv preprint doi: <https://doi.org/10.1101/2021.07.23.453541>; this version posted July 23, 2021. The copyright holder for this preprint (which was not certified by peer review) is the author/funder, who has granted bioRxiv a license to display the preprint in perpetuity. It is made available under aCC-BY 4.0 International license.

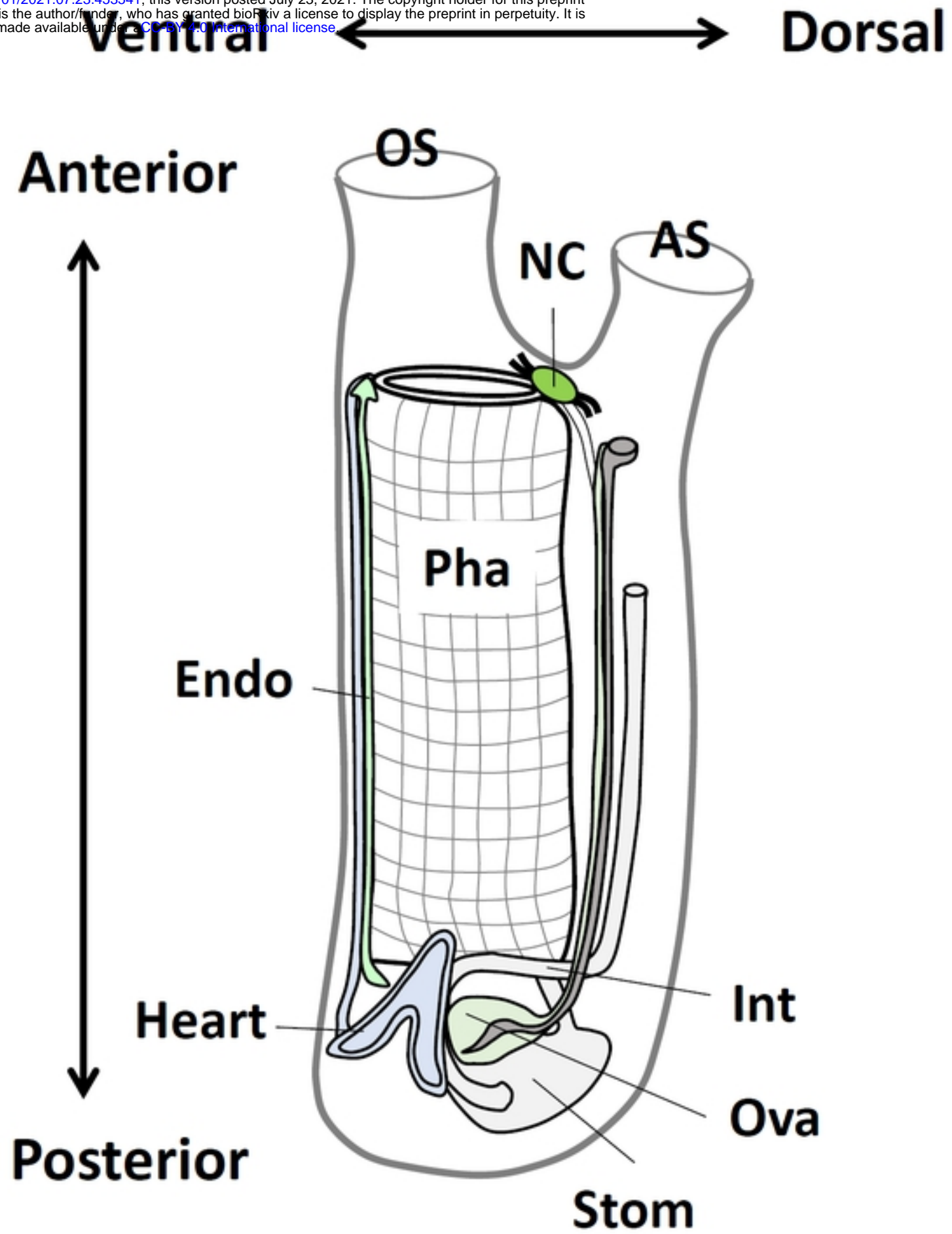




Figure 2

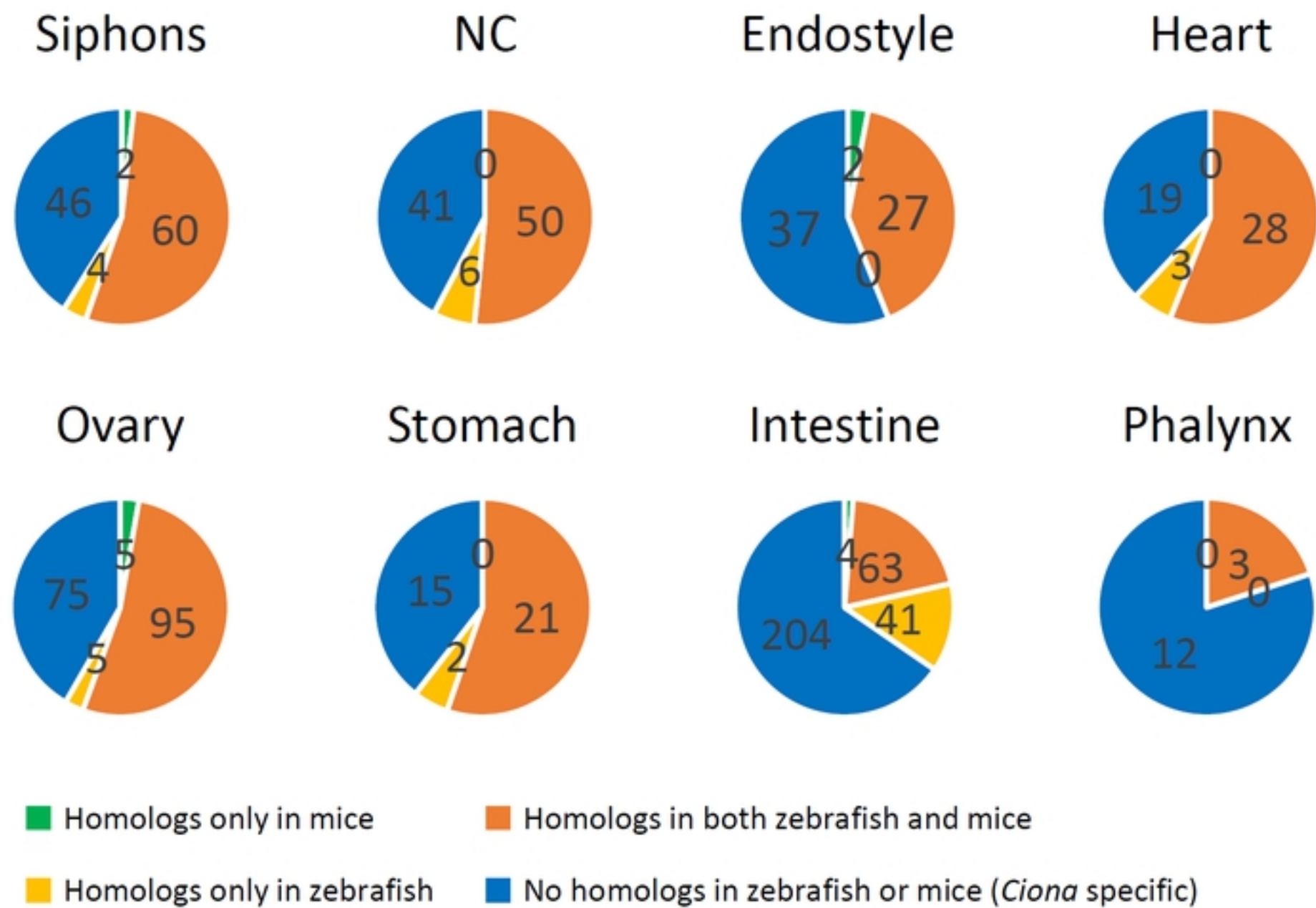
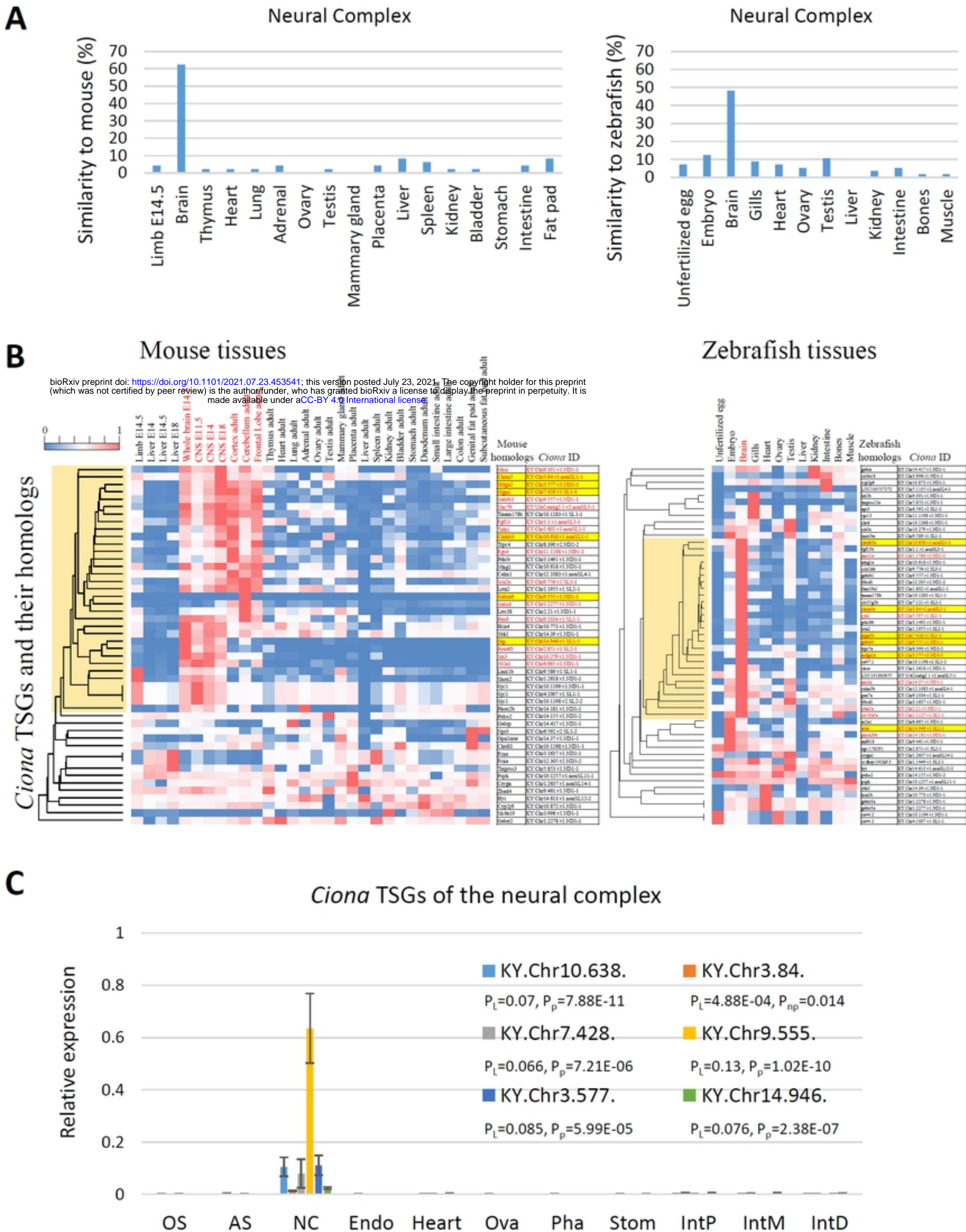


Figure 2

**Figure 3**

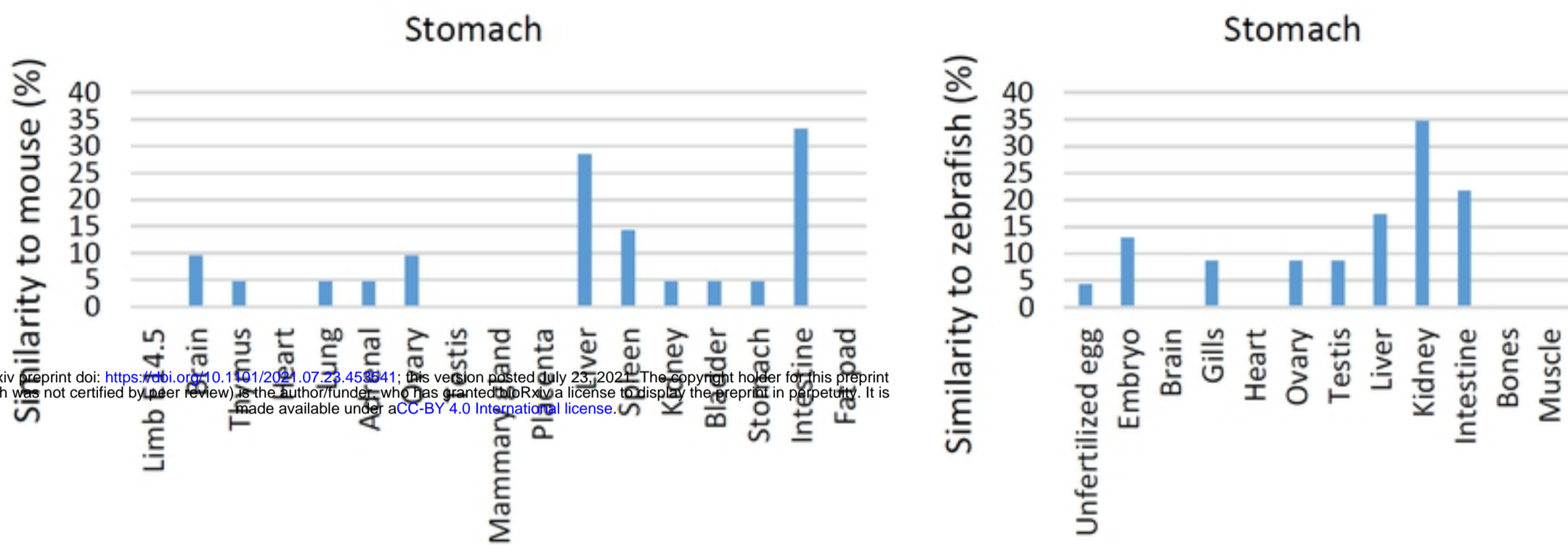


**Figure 3**



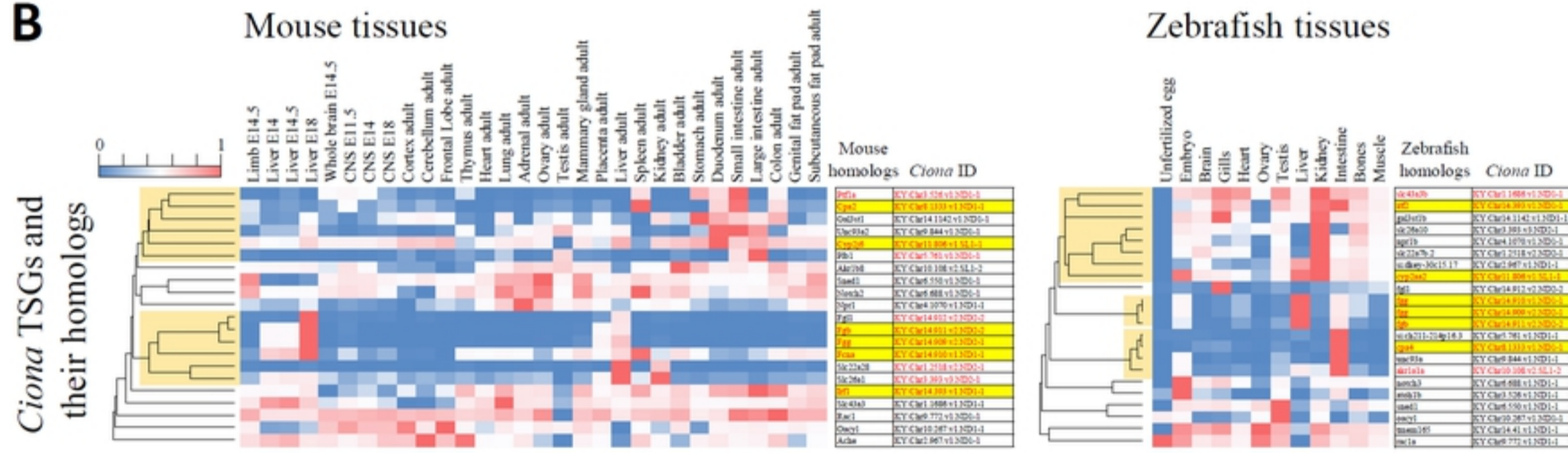
# Figure 4

## A



bioRxiv preprint doi: <https://doi.org/10.1101/2021.07.23.458341>; this version posted July 23, 2021. The copyright holder for this preprint (which was not certified by peer review) is the author/funder, who has granted bioRxiv a license to display the preprint in perpetuity. It is made available under aCC-BY 4.0 International license.

## B



## C

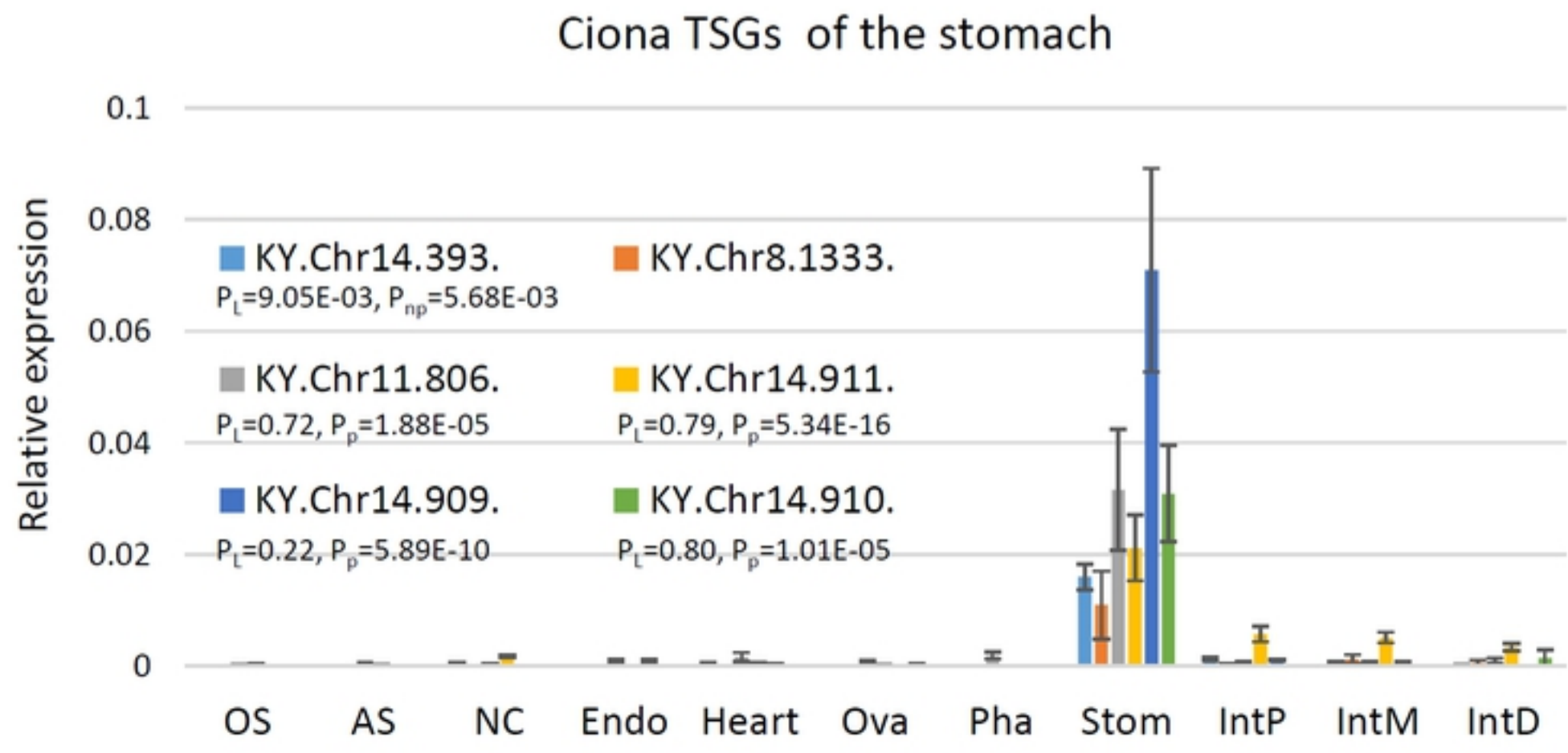
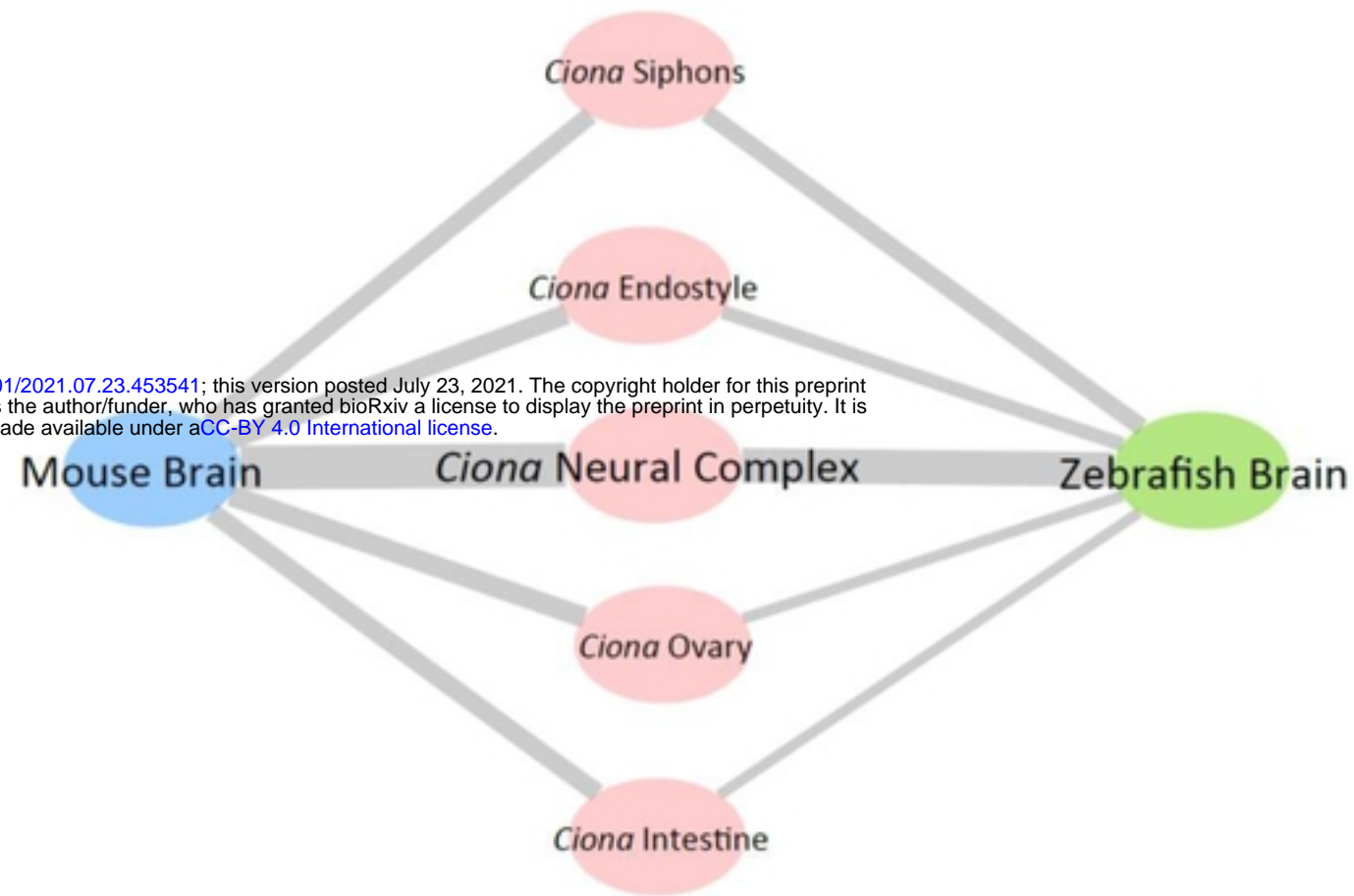


# Figure 4

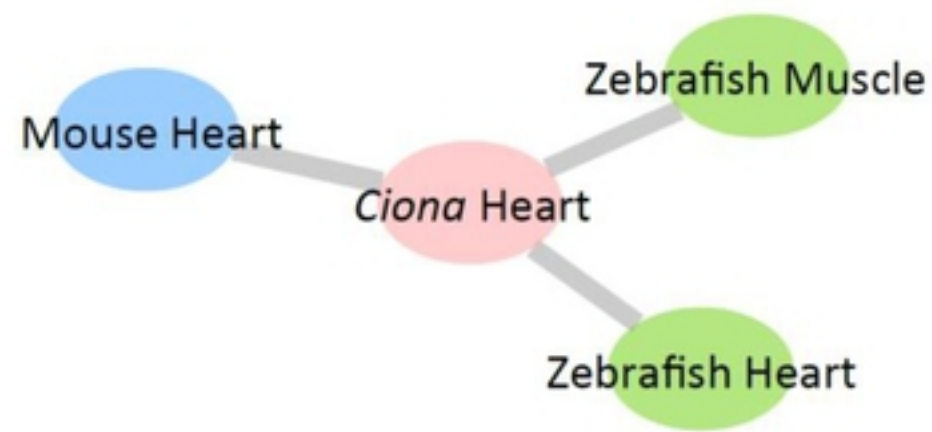
Figure 5

A

bioRxiv preprint doi: <https://doi.org/10.1101/2021.07.23.453541>; this version posted July 23, 2021. The copyright holder for this preprint (which was not certified by peer review) is the author/funder, who has granted bioRxiv a license to display the preprint in perpetuity. It is made available under aCC-BY 4.0 International license.



B



C

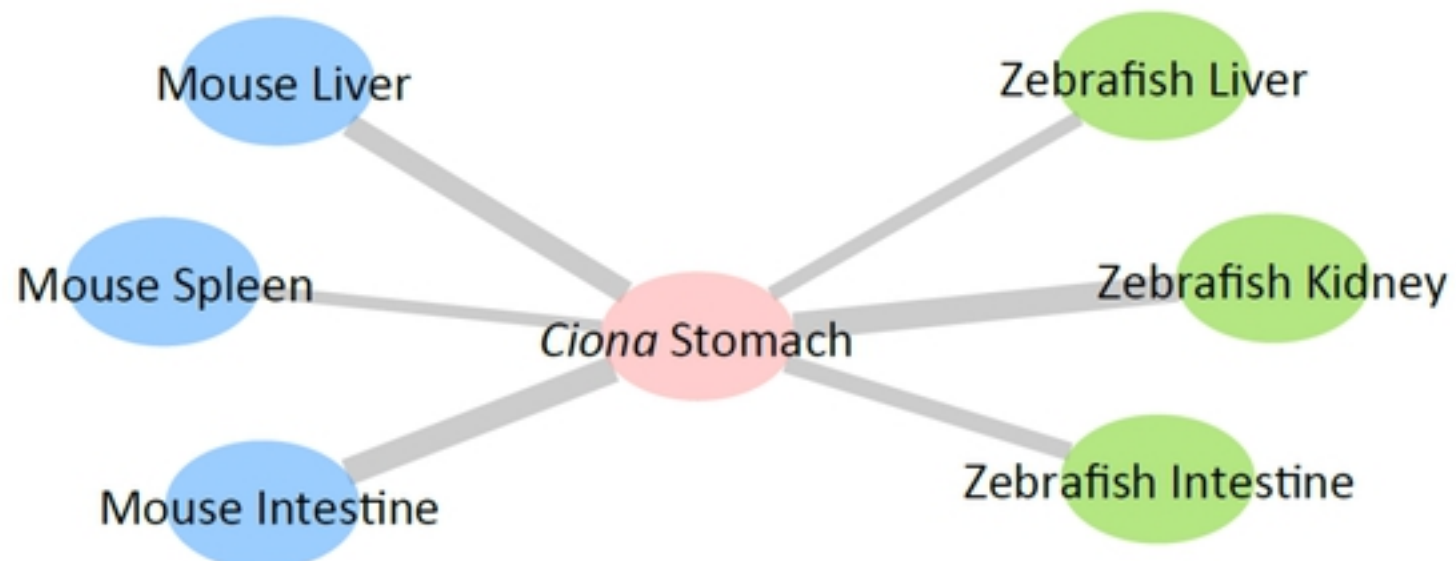


Figure 5